ISSN 0023-1584, Kinetics and Catalysis, 2010, Vol. 51, No. 3, pp. 385–393. © Pleiades Publishing, Ltd., 2010.

Heteroatom Effect on Hydrodesulphurization Activity of TiO_2-Supported Molybdenum Heteropolyoxometalates of Anderson Type[1]

A. A. Spojakina[a], E. Y. Kraleva[a], and K. Jiratova[b]

[a] *Institute of Catalysis, Bulgarian Academy of Sciences, Sofia, Bulgaria*

[b] *Institute of Chemical Process Fundamentals, Academy of Sciences of the Czech Republic, Prague, Czech Republic*

e-mail: kiyky@ic.bas.bg; mariamaleva@yahoo.ie

Received January 14, 2009

Abstract—The properties of the Mo-containing samples (6 wt % Mo) prepared by mechanochemical mixing of Fe, Co, or Ni heteropolymolybdates of Andersen type and the TiO_2 support are reported. A detailed characterization of the surface properties has been performed by BET scanning electron microscopy, IR, XPS and thermo programmed reaction methods and by testing of catalysts in the thiophene conversion. The effects of the mixing time and the nature of heteroatom on the properties of the samples are shown. The nanosized particles are formed when mechanochemical synthesis is running 30 min. The Ni-containing catalyst reveals the highest and the most stable activity compared to Co- and Fe-containing catalysts. Their hydrodesulphurization activity is compared to those of alumina and titania catalysts synthesized by the conventional impregnation method.

DOI: 10.1134/S0023158410030109

Nowadays, the need to improve the removal of sulfur from gasoline and diesel oil by means of deep hydrodesulphurization (HDS) is driven by the new environmental legislation regarding fuel specifications. Since 1960's, cobalt and molybdenum on alumina or silica are the most studied systems in HDS of petroleum fractions [1]. Many efforts are aimed to design more active HDS catalysts by either using new catalytic supports or changing the active phase [2–5]. Supported MoO_3 and other oxides of the first transition series have been widely studied as catalysts for hydrotreating processes. Recently industrial and scientific interest has focused on heteropolyoxometalates.

To date, there are few reports on the application of heteropolyacids (HPAc) in preparation of HDS catalysts [6, 7], including heteropolycompounds of Anderson type [8–10]. Heteropolycompounds can serve as a source of active components of hydrotreating catalysts. They contain both fundamental and promoting elements (heteropolyanion and countercation) in a single compound of defined structure, and therefore, their use in a study of HDS catalysts is valuable and can give useful information for further improvement of the catalysts. Initial Anderson type heteropolyoxomolybates of general formula $[XM_6O_{24}H_6]^{n-}$, where M = Mo, W and X = Co, Cr, Rh, Al, Te, Ni, are characterized by the presence of central octahedral X atom surrounded by 6 edge-sharing MO_6 octahedra showing planar hexagonal configuration [11]. The planar structure provides a close contact with the support surface.

Earlier we showed that the cobalt and nickel heteropolyoxomolybdates of Anderson type having atomic ratio Co(Ni)/Mo = 0.17, are suitable precursors of active sites for hydrotreating catalysts [8, 9]. Lately we received promising results with $CoMo/Al_2O_3$ catalyst, synthesized using CoMo heteropolyoxomolybdate of Anderson type, in the HDS of gas oil in the pilot plant catalytic unit [12].

The nature of the active phase in the prepared catalyst is determined not only by the structure of the oxide precursor species but it is strictly dependent on the preparation methods [5].

One of the important factors that affect catalyst activity is the interaction between the active components and support. The metal–support interaction plays an important role in the catalyst activity by influencing both dispersion of active ingredients and their ability to be reduced and sulfided [13, 14].

Different supports have been used for loading of HPAc. In case that HPAc are deposited on alumina their characteristic heteropolyanion structure is destroyed, and catalytic behavior of resulting catalysts is similar to that of the conventional Mo(W)-containing catalysts [7]. TiO_2 support has been reported to provide higher dispersion of the active phase [15] and

[1] The article is published in the original.

Table 1. Metal content in the HPA salts

Sample	Fe, Co or Ni, wt %	Mo, wt %	Mo/(Fe, Co or Ni), mol/mol
$FeMo_6$	4.1	43.3	6.2
$CoMo_6$	4.2	44.2	6.1
$NiMo_6$	4.6	45.8	6.1

increase the activity of CoMoS catalyst in HDS of benzothiophene [16] because heteropolycompound is kept on the support (or a newly formed compound) in a greater extent.

Method of catalyst preparation plays an important role in achieving of the optimal catalyst activity. Usage of different methods is known: impregnation, co-precipitation, sol-gel method, mechanochemical treatment [17]. Co-precipitation of the initial compounds from water solutions or impregnation of the support with the initial compounds is used to synthesize the catalysts most often. Mechanochemical treatment is less often applied in catalyst manufacture but it offers some advantages. First of all, it is simple and moreover it does not produce large quantities of waste waters etc. The positive role of the mechanochemical treatment on the HDS catalyst activity was shown earlier [18, 19]. It was also pointed out that the effect of this preparation method on the HDS activity depends on the support used [20]. The method gives especially good results when a strong acid and a base as reagents realize the interaction [21].

The goal of this paper is to study the effect of the synthesis method and the nature of heteroatom (Fe, Co, Ni) of molybdenum heteropolyoxometalates as the promoters in the TiO_2-supported HDS catalysts on their phase composition and catalytic activity in thiophene hydrodesulphurization. The catalysts were synthesized by mechanochemical mixing of the support with FeMo, CoMo, or NiMo heteropolycompounds of Anderson type. The influence of the milling time on the properties of catalysts was also examined. The results are compared with activity of conventional alumina and titama supported catalysts, synthesized by impregnation.

EXPERIMENTAL

Catalyst Preparation

The catalysts were prepared by mechanochemical mixing of the TiO_2 support and the Fe, Co, or Ni heteropolymolybdates of Anderson type in an agate mortar for 30 and 90 min. The laboratory synthesized TiO_2 has anatase structure, $S_{BET} = 72$ m^2/g, and pore volume 0.198 cm^3/g. Commercial product $[(NH_4)_3Fe(OH)_6Mo_6O_{18}$ salt ("Chimreactiv," Russia, pure) and $[(NH_4)_3Co(OH)_6Mo_6O_{18}]$ and $[(NH_4)_4Ni(OH)_6Mo_6O_{18}]$ salts, synthesized in our laboratory according to [22, 23] were used for the catalyst preparation. The salts are denoted as $FeMo_6$, $CoMo_6$, and $NiMo_6$, respectively. The composition of all salts is presented in Table 1. The composition of the synthesized heteropolycompounds is close to the theoretical one. Amounts of the loaded salt and the support were chosen intentionally in order the amount of molybdenum in all catalysts was 6 wt %. The milled catalysts were dried 4 h at 105°C and calcined 2 h at 350°C. Denotion of the catalysts includes both the abbreviation of the used salt ($FeMo_6$, $CoMo_6$, $NiMo_6$) and the time of treatment (30, 90), e.g., $FeMo_6$-30 means that the $(NH_4)_3Fe(OH)_6Mo_6O_{18}$ salt is mixed with the TiO_2 support for 30 min in the mortar.

Catalysts Characterization

Specific surface area. The surface area of the catalysts was determined from the nitrogen adsorption–desorption isotherms at –195°C (BET method).

Scanning electron microscopy (SEM). Scanning electron microscope JSM-5300 ("Jeol") was used to study the morphology of the deposited layers in oxidic form. The photographs were taken in the regime of secondary electrons (SEI).

Temperature-programmed reduction (TPR). TPR measurements were carried out in an apparatus described earlier [24]. Hydrogen/nitrogen mixture (10 mol % H_2) was used to reduce catalysts at a flow rate of 17 cm^3/min. The temperature was linearly raised at a rate of 20°C/min up to 850°C.

IR spectra. IR spectra (400–1200 cm^{-1}) were recorded at room temperature on a "Bruker IFS-25 Fourier transform" IR spectrometer. The catalysts were pressed with KBr in ratio 1 : 150. Alumina and titama absorption in the 400–1200 cm^{-1} range was compensated by subtraction of a normalized spectrum of the equivalent amount of support from the catalyst spectrum [25].

X-ray photoelectron spectroscopy (XPS). XPS measurements were performed with "ESCALAB-Mk II" ("VG Scientific") electron spectrometer at a base pressure 1×10^{-8} Pa.

Samples were excited with MgK_α radiation ($h\nu$ = 1253.6 eV). The total energy resolution of the instrument was 1.2 eV as measured by half width of the Ag $3d_{5/2}$ photoelectron peak. Powdered samples were pressed into 12 mm diameter stainless-steel sample holders to obtain a thickness of 0.7–1 mm. After introduction into the preparation chamber of the electron spectrometer, samples were evacuated to and transferred to the analysis chamber for XPS measurements. The glass reactor with sulfided sample was opened in a glove box connected to the fast entry lock of the XPS instrument. The sample was transferred to its holder without exposure to air. The following photoelectrons

Table 2. Catalysts characteristics

Parameter*	Catalyst					
	$FeMo_6$-30	$FeMo_6$-90	$CoMo_6$-30	$CoMo_6$-90	$NiMo_6$-30	$NiMo_6$-90
S_{BET}, m^2/g	68.4	53.3	58	62.3	53.6	60.2
V_{micro}, mm^3/g	1.6	12.3	1.5	13.2	0.6	1.4
S_{meso}, m^2/g	67.0	32.3	56.2	40.5	53.8	58.5
V_{total}, cm^3/g	0.20	0.15	0.20	0.19	0.19	0.18
C_{modif}	90	12	90	12	100	100
d, nm	10.3	9.7	11.6	11.0	12.6	11.2
d_{max}, nm	10	9.5	7	8.4	7.5	8.12

* Total pore volume V_{total} was calculated from Barrett–Joiner–Halenda (BJH) equation; constant C_{modif} calculated from modified BET equation [27]; the volume of micropores V_{micro} expressed in mm^3 of liquid N_2 on gram of catalyst.

were recorded: C 1*s*, O 1*s*, Mo 3*d*, Ti 2*p*, Fe 2*p*, Co 2*p*, Ni 2*p*, and S 2*p*.

The binding energies (BE) of C 1*s*, O 1*s*, Mo 3*d*, Ti 2*p*, Fe 2*p*, Co 2*p*, Ni 2*p*, and S 2*p* core electron levels were determined by computer fitting the measured spectra and were referenced to the C 1*s* XPS signal at 284.5 eV. The binding energy was taken at the Ti 2*p* at 458.5 eV an estimated error of 0.1 eV can be assumed for all the measurements. In order to obtain information on the surface structure and the dispersion of the active phases the surface atomic ratios were calculated as the ratio of the corresponding peak intensities, corrected with theoretical sensitivity factors based on Scofield's photoionization cross-sections [26].

Catalytic Activity

HDS of thiophene was carried out in a continuous flow reactor at 350°C and 0.1 MPa. Each experiment was carried out with a fresh catalyst (0.1 g) that was standardized by in situ calcination (30 min) in argon at 350°C. The calcined catalyst was activated by sulfidation with a mixture of $H_2S + H_2$ during 1 h at 350°C and flow rate 40 cm^3/min. We have found out in our preliminary experiments that this sulfidation treatment gives maximal catalytic activity of the catalysts. After the activation of the catalyst had been completed, the catalyst was flushed (30 min) with argon at the same temperature, and then, the reaction mixture (6 mol % of thiophene in hydrogen) with weight hour space velocity (WHSV) of thiophene 2 h^{-1} was fed into the reactor. Activity of the catalyst has been measured for 5 h. It was expressed as the thiophene conversion to C_4 hydrocarbons.

RESULTS AND DISCUSSIONS

Specific Surface Area and Porous Characteristics

Specific surface areas (S_{BET}) and porous characteristics of the catalysts are presented in Table 2.

Average diameter of pores d is calculated from pore volume V_{total} and surface area S_{BET} as $d = 4V_{total}/S_{BET}$. The values V_{micro}, S_{meso}, and C_{modif} were calculated from modified BET equation [27]. It takes into account capillary condensation of nitrogen in micropores (<2 nm); that is why the volume of micropores is given in mm^3 of liquid nitrogen on g. Diameter of pores d_{max} is given by a maximum in desorption curves of nitrogen.

It is seen that the specific surface area of the catalysts prepared by mechanochemical treatment in comparison with the support surface decreases depending on the composition of the samples and time of milling.

Differences in the C constants of the BET equation for both the $FeMo_6$ and $CoMo_6$ samples in comparison to the $NiMo_6$ sample indicates changes in the state of their surface after long mechanochemical treatment. Also micropore volume V_{micro} of the Fe- and Co-containing catalysts increases more significantly after the long mechanochemical treatment. The surface of mesopores S_{meso} decreases for these samples whereas it increases slightly for the $NiMo_6$ sample. Any change in the pore volume V_{total} is practically not observed with all samples except the $FeMo_6$ one, where the longer time of treatment decreases V_{total}.

We suppose some reasons of the decrease in the specific surface area of the mechanochemically treated samples. Most probably, it is the result of the local overheating of the supporting phase, its migration and blockage of the pores. The plastic deformation which the catalyst samples undergo during the mechanochemical treatment induce a number of nonsteady-state processes, appearance of defects and/or destruction of the crystal lattice, variation in the form and the size of the particles, changes in the specific surface area and in the porosity. The energy accumulation in defects in the new phases increases the temperature and stimulates a transformation of the new phases in other ones with a lesser surface.

The high homogenization of the mixture of interacted components helps to mechanochemical synthe-

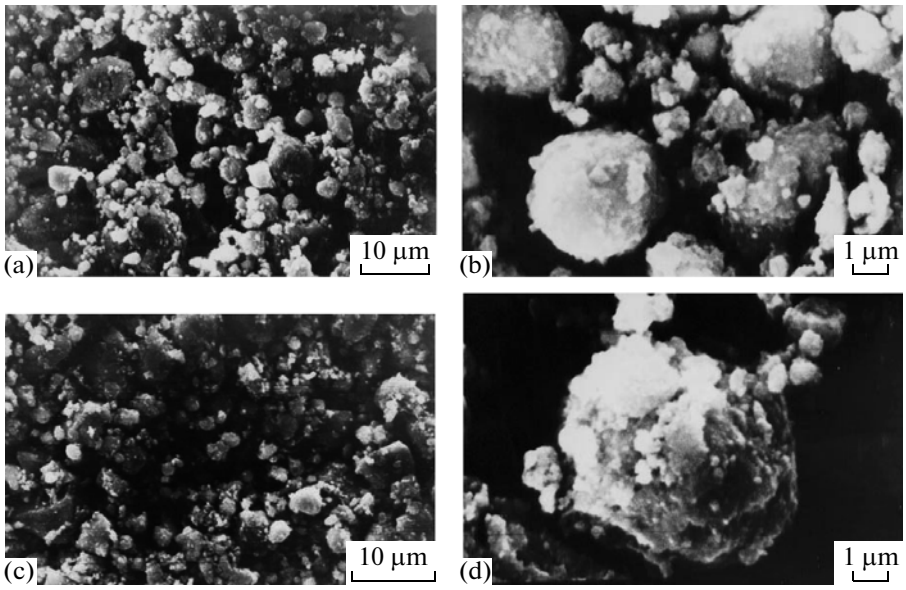

Fig. 1. SEM photography of the catalysts: (a), (b) $CoMo_6$-30; (c), (d) CoMo6-90.

sis. The hydration water separated from loaded heteropolycompound is retained in the volume of the mixture and most probably, plays an important role in the new phases formation (specifically, new heteropolycompounds) or their partial conservation. It was mentioned earlier that mechanochemical synthesis proceeds more easily when acid-base interaction can proceed. In that case sorption ability of a support is increasing [17, 28]. Along with high dispersion of the mixture the dense aggregates are formed during the mechanochemical treatment. Interior of these aggregates can be inaccessible for the surface area measurement. Chemical composition of the catalysts affects the porous structure and surface properties. Low concentration of the components likely helps to formation of these dense aggregates [29].

SEM Microscopy

SEM microscopy can reveal changes in morphology of the catalysts depending on the treatment time. Pictures presented in Fig. 1 belong to the $CoMo_6$ catalysts, which were chosen as an example, treated for different time. Formation of layers and the size increase of the particles growing on the layers after longer time of treatment can be seen. Apart from the bigger particles a great number of nanosized particles remains on the layers. No change in the form of these particles is observed.

IR Spectroscopy

In the IR spectrum of the initial ammonium Fe, Co, Ni polyoxomolybdates the bands at about 944, 926, 890, 645, 572 cm^{-1} characteristic for Anderson type heteropolycompound are revealed. In the region 1400–1650 cm^{-1}, the OH^- and N–H bending can be registered; the central Mo–O–(Al, Co, Ni) stretching is revealed around 550 cm^{-1} [30] (Fig. 2).

It should be noted that no difference in the IR spectra of the samples treated 30 and 90 min has been revealed. In the catalysts spectra, the large band in the region 960–800 cm^{-1} is observed which is related to the bridge bond Mo–O–Mo and terminal $Mo{=}O_t$.

The OH bending vibrations of low intensity at around 1625 cm^{-1} are detected. These bands are observed due to the water presence in the synthesized catalyst. The result shows the presence of heteropolyanions on the surface. No MoO_3 phase is present in the catalysts (bands at about 880 and 990 cm^{-1} are absent).

The characteristic bands of the initial salts at 944, 926, 890 cm^{-1} transforms in a new large band at 960–800 cm^{-1}, i.e., the loaded salts are transformed morphologically in significantly anhydrous amorphous phases in which the Anderson anion is present but the symmetry connected with the crystallized water is destroyed. The symmetry connected with the hydration water in the initial salt is lost as a result of its interaction with the support. In the region 400–800 cm^{-1} of all catalysts spectra the new band at ~725 cm^{-1} is detected. New bands at about 625 and 530 cm^{-1} can be seen in the spectra of Fe- and Co-containing catalysts whereas in the spectrum of the $NiMo_6$ these bands can be distinguished only slightly. The new band at 670 cm^{-1} appeared in the spectra of Co- and Ni-containing samples, not in the spectrum of $FeMo_6$ catalyst. Assignment of the new bands is problematic. We suggest that they can be associated with some type of interaction of the initial heteropolycompounds with the support. New compounds with a distorted struc-

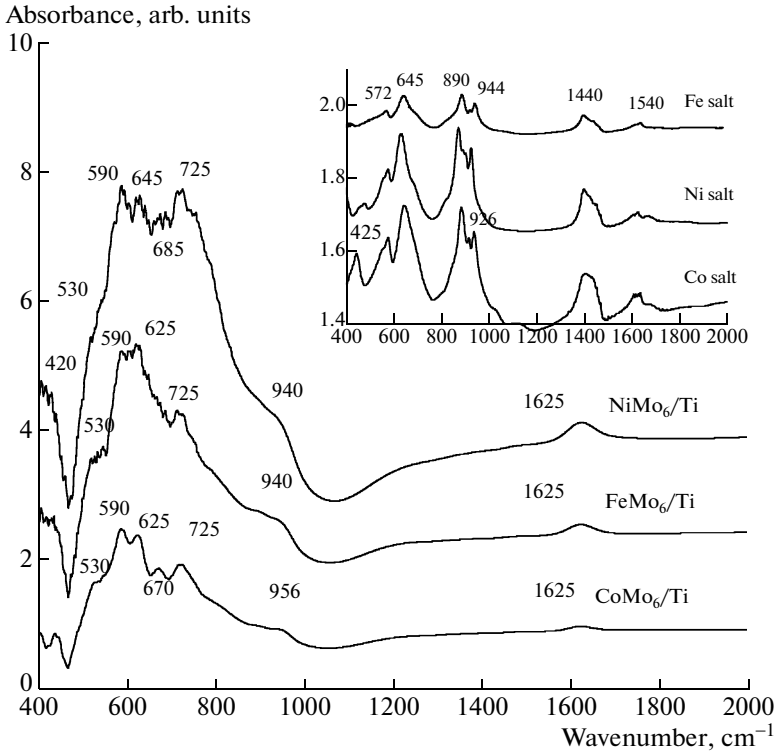

Fig. 2. IR spectra of the initial Co, Fe, Ni salts and of corresponding catalysts.

ture are likely formed on the surface of the catalysts as a result of mechanochemical treatment and interaction between components of the mixture.

Formation of different molybdenum compounds having polymeric structure is also possible. Along with the amorphous anhydrous phase of initial heteropolycompounds new molybdenum isopolycompounds and heteropolycompounds could be formed. Broadening of the bands in this region as well as shifting to a bond of weaker strength confirms distortion of the heteropolycompounds and their interaction with the support.

TPR Method

The TPR profiles of the initial salts and those supported on TiO_2 show effect of the heterocation and support on their reduction (Fig. 3). In the TPR profiles of the initial compounds, three principle maxima at 450–470, ~680, and >800°C are observed. The profiles of Fe and Co salts are similar but that one of Ni salt differs appreciably.

Two strong peaks appearing in the reduction patterns of the initial salts are attributed to Mo(VI) → Mo(IV) and Mo(IV) → Mo^0 reduction steps [31]. Comparing the patterns we could see that reduction of the salts starts at about 300°C, the first peak of the $NiMo_6$ salt being appeared at lower temperature and probably includes the Ni heteroatom reduction, which is close to the reduction of Ni^{2+} ions in the NiO phase [32]. Reduction of Fe heteroatom in $FeMo_6$ is indicated only slightly at around 605°C. Compared to reduction of $NiMo_6$, both strong reduction peaks of the $FeMo_6$ and $CoMo_6$ salts are shifted to higher temperatures documenting the promoting role of Ni in the reduction steps. Very little gap between two strong peaks in these samples permits to support the formation intermediate phase including the Fe^{3+} and Co^{3+} in agreement with the authors of the paper [31].

After loading of the salts over the titania support their TPR profiles are changed (Fig. 3, the only pictures for the samples treated 30 min are presented). The peaks are enlarged as a result of the salt interaction with the support and the phase heterogeneity. The part concerning the reduction of the support at about 600°C is possible [15] but it is overlapped with the peaks connected with reduction of other phases. Two peaks with the suggested gap between them are observed with all examined catalysts. In the picture of the $NiMo_6$ catalyst, the first peak has clearly noticeable shoulder which is separated from the second peak of lower intensity.

The low-temperature peaks (at 438–516°C) in the profiles of the catalysts is associated with the reduction of Mo^{6+} to Mo^{4+} of polymeric octahedral Mo species in the heteropolycompounds where Mo has the octahedral coordination and more easily reducible. The presence of the nickel in the $NiMo_6$ sample decreases the T_{max} of the first peak and increases the H_2 con-

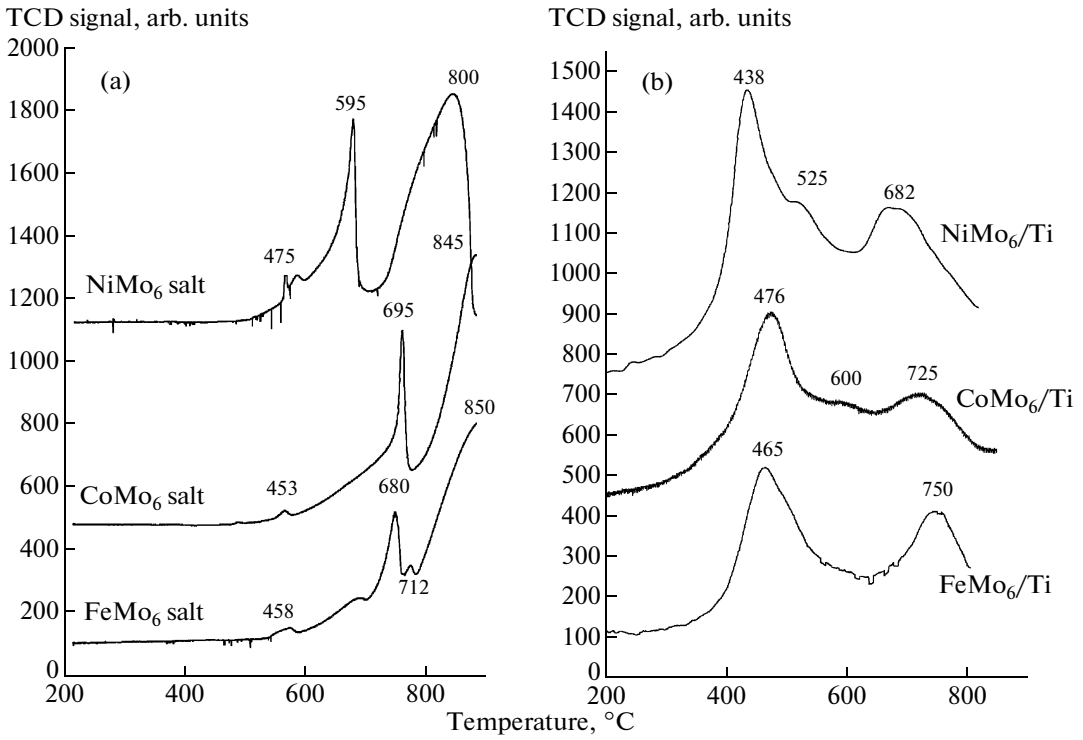

Fig. 3. TPR profiles of the initial salts (a) and catalysts after 30 min mechanochemical treatment (b).

sumption simultaneously. The presence of the initial and/or the newly formed heteropolycompounds was shown in the IR spectra of the samples (see Fig. 2). The low intensive peak at 525°C at the TPR profile of this sample could be reveal reduction of a formed mixed compound. The second enlarged high-temperature peak reveals further reduction of the compounds formed. If we compare the TPR data obtained with the catalysts mechanochemically treated for different time (T_{max} are presented in Table 3) we detect slower reduction of the catalysts treated for 90 min, especially in the low temperature range (e.g., the T_{max} of the first peaks of the $FeMo_6$ catalyst treated for 30 and 90 min are ~450 and 512°C, respectively). The observation can be connected with bigger particles formed during long mechanochemical treatment what is confirmed by the SEM results in which layers and bigger particles were identified (see Fig. 1).

XPS Method

XPS method has been used to study the element states of oxidic and sulfided forms of the catalysts. The results for the Mo $3d_{5/2}$ XPS spectra are presented in the Fig. 4. The XPS data are presented only for the samples mechanochemically treated for 30 min because no substantial differences in the spectra of the samples treated for 90 min is observed. The difference can be expected only in the number of the Mo species of the same type.

The molybdenum in oxidic form of the catalysts appears with BE of 232.5 eV (Fig. 4a). Decompositions of the spectra reveal the only doublet with BE Mo $3d_{5/2}$ of 232.5 eV related to Mo^{6+} octahedral coordination. The finding is in accord with the Mo state in the surface polymolybdate phases.

These XPS spectra change after sulfidation of catalysts. The spectrum of the titania supported catalysts sulfided 1 h reveals two doublets with binding energy

Table 3. TPR profiles of the examined catalysts*

Parameter	Catalysts					
	$FeMo_6$-30	$FeMo_6$-90	$CoMo_6$-30	$CoMo_6$-90	$NiMo_6$-30	$NiMo_6$-90
T_{max}, °C	465; 750	512; sh 718; 769	475; 590; 726	489; 789	435; sh 519; 680	413; 576; 710
mmol H_2/g (20–800°C)	1.59	1.40	1.31	1.10	2.30	2.10

Note: * sh = shoulder.

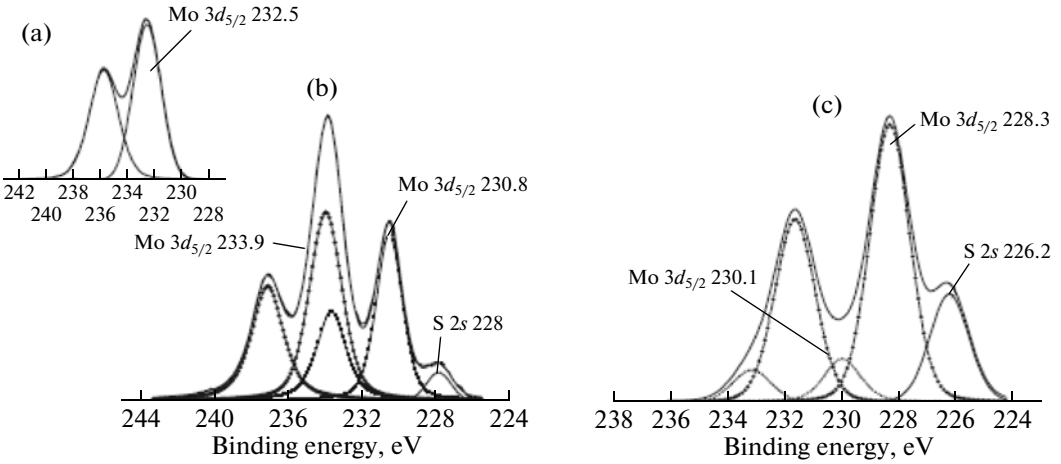

Fig. 4. XPS spectra of the $FeMo_6$ catalyst in various form: (a) oxidic, (b) sulfided ($H_2 + H_2S$, 1 h), (c) after reaction.

233.9 and 230.8 eV (Fig. 4b). We suggest that the first doublet is related to Mo^{6+}(Td) and the second to Mo^{5+}. Very likely, Mo^{6+}(Td) is included in the iron, cobalt and nikel molybdate phase while Mo^{5+} species are connected with polymolybdate structures where Mo^{5+} species are situated in the sulfided Ni(Co, Fe)-Mo polymeric phase forming oxysulfides [33–35]. We cannot expect any MoS_2 phase formation after 1 h catalyst sulfidation with the $H_2 + H_2S$ mixture, because the XPS did not reveal any Mo^{4+}-ions.

Comparison of the XPS spectrum of the fresh catalyst with that of the catalyst after reaction shows change in the molybdenum state (Fig. 4c). The spectrum fitting reveals two doublets with binding energy 228.3 and 230.1 eV what indicates formation of the MoS_2 phase and presence of Mo ions in the Mo^{4+} state [36–38] and some amount of Mo^{5+} species in fully sulfided or/and in the MoS_x phase.

In the spectra of the sulfide catalysts the peak of S 2*s* with binding energy 226.7 eV is revealed. It is ascribed to S^{2-} appearing from adsorbed H_2S.

Based on the XPS results, iron in the oxidic and sulfided forms of the catalysts exists as Fe^{3+} (BE = 709.7 eV) (the spectra are not presented).

The XPS spectra of cobalt and nickel in both the $CoMo_6$ and $NiMo_6$ catalysts are of low intensity and therefore the state of both metals cannot be determined.

Hydrodesulphurization Activity

Hydrodesulphurization activity of the catalysts, related to 1 mol of Mo, was evaluated from thiophene conversion (Fig. 5). The HDS activity of the support is about 3 mol %.

It is clear from Fig. 5 that the kind of captions in the initial polyoxometalates and the time of the mechanochemical treatment affect the thiophene conversion. The cation influence on the activity and stability of the catalysts depends on the time of milling. The initial activity of all catalysts treated for 30 min is the same and it is higher than the activities of the catalysts treated 90 min. The high initial activity of the $FeMo_6$-30 quickly decreases with increasing time on stream. When the Fe containing sample is milling 90 min its activity is stable. The order of the catalyst activities however remains constant regardless the time of mechanochemical treatment.

Higher activity of the shortly treated catalysts can be likely ascribed to formation of active phase monolayer covered with separated nanoparticles of the active phase. A decrease in the value of the steady state activity with increasing mechanochemical treatment time could be connected with destruction of the layers of the catalysts, particles packing and their agglomeration. Thus, treatment process used during catalyst

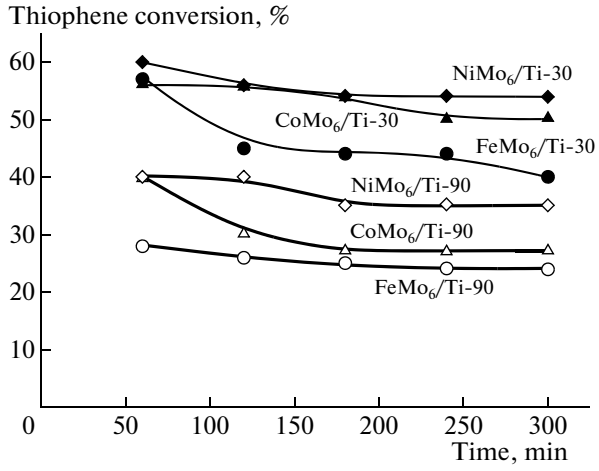

Fig. 5. Thiophene conversion over the catalysts treated for 30 and 90 min and sulfided for 1 h (conversion is related to 1 mol Mo).

preparation likely results in a decrease in the number of active sites on the catalyst surface.

The Ni containing samples treated 30 and 90 min are the most active and stable in comparison to other samples.

The decrease of catalyst activity with time of stream can be connected with the formation of less active phase, probably with the MoS_2, which was not revealed after sulfidation of the catalysts (see comment to XPS data in this paper) but which could be formed as a result of sulfidation by H_2S formed during HDS of thiophene. We showed earlier that activity depends on the Mo^{5+}/Mo^{4+} ratio and it is higher when Mo^{5+} prevails [15, 39]. The HDS catalyst activity is diminished when this ratio decreases as result of the MoS_2 formation during increasing time of stream. Higher activity of the $NiMo_6$ catalyst is connected with stabilizing action of nickel and its participation in the formation of the separated active phase that begins to reduce at lower temperature.

Comparison of the HDS activity of the samples under investigation (Fig. 5) with that of alumina and titania supported catalysts prepared by impregnation method shows their close or higher activity: thiophene conversion on the $CoMo/Al_2O_3$ industrial catalyst (13.7 wt % Mo and 2.4 wt % Co) at 350°C is 45 and 23 mol % at WHSV of 1 and 3 h^{-1}, respectively, [12] and thiophene conversion on the $FePMo_6$ catalyst (TiO_2 support, 6 wt % Mo and 0.25 wt % Fe) is about 37 mol % at 2 h^{-1} and 350°C [15].

The results obtained show that nanosized particles are formed during mechanochemical synthesis (30 min of mixing) of the HDS catalysts. Their HDS activity is affected by presence of the heterocation, the maximum activity can be reached when optimum interaction between active phase and support is realized providing formation of the nanosized particles. Nickel in the titania supported $NiMo_6$ catalyst shows specific effect. The $NiMo_6$ catalyst reveals the highest and the most stable activity compared to both $CoMo_6$ and $FeMo_6$ catalysts. The activities of the HDS catalysts under investigation are close or higher in comparison to those of the alumina and titania supported catalysts prepared by impregnation method.

ACKNOWLEDGMENTS

The authors would like to thank Bulgarian and Czech Academies of Sciences for the support of the research in the joint project. E.K. thanks for the financial support the Bulgarian Ministry of Education, Fund "SCIENTIFIC RESEARCH" (project postdoc no. D01-900 11/07).

REFERENCES

1. Topsøe, H., Clausen, B.S., and Massoth, E.F., *Hydrotreating Catalysts: Science and Technology*, Berlin: Springer, 1996.
2. Zepeda, T.A., Pawelec, B., Fierro, J.L.G., and Halachev, T., *J. Catal.,* 2006, vol. 242, p. 254.
3. Ma, X.L., Sakanishi, K., and Mochida, I., *Ind. Eng. Chem. Res.*, 1996, vol. 35, p. 2487.
4. Topsøe, H. and Clausen, B.S., *Cat. Rev. Sci. Eng.,* 1984, vol. 26, p. 395.
5. Clausen, B.S., Topsøe, H., Candia, J., Lengeler, B., and Alsnielsen, J., *Bull. Soc. Chim. Belg.*, 1981, vol. 90, p. 1249.
6. Spojakina, A., Jiratova, K., Kostova, N., Kocianova, Y., and Stamenova, M., *Kinet. Catal.,* 2003, vol. 44, p. 886.
7. Griboval, A., Blanchard, P., Payen, E., Fournier, M., and Dubois, J.L., *Catal. Today,* 1998, vol. 45, p. 277.
8. Spojakina, A.A., Gigov, B., and Shopov, D.M., *React. Kinet. Catal. Lett.*, 1982, vol. 19, p. 11.
9. Spojakina, A.A., Kardjieva, R., Damyanova, S., and Shopov, D.M., *Proc. V Int. Symp. on Heterogeneous Catalysis*, Varna, 1983, part II, p. 353.
10. Cabello, C.I., Munoz, M., Botto, I.L., and Payen, E., *Thermochim. Acta,* 2006, vol. 447, p. 22.
11. Perloff, A., *Inorg. Chem.,* 1970, vol. 9, no. 10, p. 2228.
12. Spojakina, A., Jiratova, K., Novak, V., Palcheva, R., and Kaluza, L., *Collect. Czech. Chem. Commun.*, 2008, vol. 73, p. 983.
13. Gutierrez-Alejandre, A., Ramirez, J., Jimenez-del, Val. V.I., Penuelas-Galaz, M., Sanchez-Neri, P., and Torres-Mancera, P., *Catal. Today,* 2005, vol. 107/108, p. 879.
14. Grzechowiak, J.R., Wereszczako-Zielinska, I., Rynkowski, J., and Ziolek, M., *Appl. Catal., A*, 2003, vol. 250, p. 95.
15. Spojakina, A., Kraleva, E., Jiratova, K., and Petrov, L., *Appl. Catal., A*, 2005, vol. 288, p. 10.
16. Tanaka, H., Boulinguiez, M., and Vrinat, M., *Catal. Today,* 1996, vol. 29, p. 209.
17. Gaffet, E., Bernard, F., Niepce, J., Charlot, F., Gras, C., Le Caer, G., Guichard, J., Delcroix, P., Mocellin, A., and Tillement, O., *J. Mater. Chem.*, 1999, vol. 9, p. 305.
18. Andonova, S., Vladov, Ch., Kunev, B., Mitov, I., Tyuliev, G., Fierro, J.L.G., Damyanova, S., and Petrov, L., *Appl.Catal., A,* 2005, vol. 298, p. 94.
19. Kouzu, M., Uchida, K., Kuriki, Y., and Ikazaki, F., *Appl.Catal., A*, 2004, vol. 276, p. 241.
20. Kostova, N., Kraleva, E., Spojakina, A., Godocikova, E., and Balaz, P., *J. Mater. Sci.*, 2007, vol. 42, p. 3321.
21. Mestol, G. and Knozinger, H., *Langmuir*, 1998, vol. 14, p. 3964.
22. Friedheim, K. and Keller, F., *Ber. Dtsch. Chem. Ges.,* 1906, vol. 39, p. 430.
23. Nikitina, E.A., *Geteropolisoedineniya* (Heteropoly Compounds), Moscow: Goshimizdat, 1962.
24. Solcova, O., Uecker, D.Ch., Steinike, U., and Jiratova, K., *Appl. Catal., A*, 1994, vol. 94, p. 153.
25. Davidov, A. and Goncharova, O., *Usp. Khim.*, 1993, vol. 62, p. 105.
26. Scofield, H.J., *J. Electron Spectrosc. Relat. Phenom.*, 1976, vol. 8, p. 129.
27. Schneider, P., *Appl. Catal., A*, 1995, vol. 129, p. 157.

28. *Polyoxometalates: From Platonic Solids to Antiretroviral Activity*, Pope, E.M.T. and Muller, A., Eds., Dordrecht: Kluwer, 1994.
29. Segawa, K. and Hall, W.K., *J. Catal.,* 1982, vol. 76, p. 133.
30. Botto, I.L., Garcia, A.C., and Thomas, H.J., *J. Phys. Chem. Solids*, 1992, vol. 53, p. 1075.
31. Cabello, C.I., Botto, I.L., and Tomas, H.J., *Thermochim. Acta,* 1994, vol. 232, p. 183.
32. Mangnus, P.J., Bos, A., and Moulijn, J.A., *J. Catal.,* 1994, vol. 146, p. 437.
33. Weber, Th., Muijsers, J.C., van Wolput, J.H.M.C., Verhagen, C.P.J., and Niemantsverdriet, J.W., *J. Phys. Chem.*, 1996, vol. 100, p. 14144.
34. Weber, Th., Muijsers, J.C., and Niemantsverdriet, J.W., *J. Phys. Chem.*, 1995, vol. 99, p. 9194.
35. Abart, J., Delgado, E., Ertl, G., Jeziorowski, H., Knozinger, H., Tiele, N., Wang, X., and Tagloaer, E., *Appl. Catal.,* 1982, vol. 2, p. 155.
36. Quincy, R., Houalla, M., Proctor, A., and Hercules, D., *J. Phys. Chem.*, 1990, vol. 94, p. 1520.
37. Zingg, D., Makovsky, L., Tischer, R., Brown, F., and Hercules, D., *J. Phys. Chem.*, 1980, vol. 84, p. 2898.
38. Spevack, P.A. and McIntyre, N.S., *J. Phys. Chem.*, 1993, vol. 97, p. 11020.
39. Spojakina, A. and Kostova, N., *Stud. Surf. Sci. Catal.*, 1994, vol. 88, p. 651.